Calculation of Structures and Bond Dissociation Energies of Radical Cations: The Importance of Through-Bond Delocalization in Bibenzylic Systems[1,2]

Donald M. Camaioni

Contribution from Batelle, Pacific Northwest Laboratories, P.O. Box 999, Richland, Washington 99352. Received February 15, 1990. Revised Manuscript Received August 14, 1990

Abstract: Structures and energies (ΔH°_f of radical cations and their radical and cationic fragments have been calculated by use of AM1 semiempirical molecular orbital theory and compared with experimental data in the literature. Experimental ΔH°_f correlate linearly with calculated heats giving nonzero intercepts and nonunit slopes. The best correlations as judged by the variance of the fit are obtained when performed according to structure types, i.e., aromatic radical cations, alkane radical cations, radicals, and cations. These correlations enable corrections to AM1 values that allow prediction of experimental ΔH°_f with uncertainties that approach experimental uncertainties. Used in this way, AM1 can augment experimental thermochemical data and enable confident predictions of reaction enthalpies. Bibenzylic radical cations are calculated to have charge and spin localized in only one of the aromatic rings in their lowest energy conformations. No minima for bibenzylic structures with delocalization between the aromatic rings either through space or through the ethylenic bond are found. Reaction paths for scission of radical cations are judged to be differentiated by whether the scissions are endothermic or exothermic. Endothermic scissions, such as for bibenzyl radical cation, are predicted to be loose, late-transition states. Barriers to recombination are negligible, and bonding interactions occur over relatively large distances. Exothermic scissions, such as for bicumyl radical cation, conversely are calculated to have tight, early-transition states. Structures with through-space delocalization appear to be important models for transition states of exothermic fragmentation reactions of radical cations, i.e., fragmentation of bicumyl radical cation to cumyl cation and cumyl radical.

C–C bond cleavage is a common and well-documented result of one-electron oxidative[2-9] and photochemical processes[10-15] that generate transient radical cations. This evidence as well as that from organic mass spectrometry[16] strongly suggests that certain bonds in radical cations are substantially weaker compared to their neutral counterparts. Thus, polar reaction pathways involving radical-cation intermediates would appear to be attractive alternatives to homolytic pathways for cleaving bonds and as such could provide new and possibly better processes for converting coal to chemicals and fuels.[17,18] Radical-cation pathways may

Scheme I
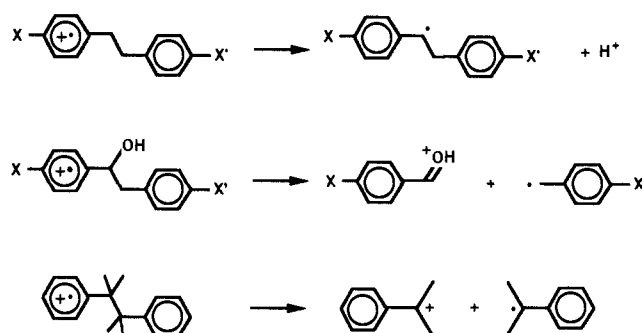
Scheme II
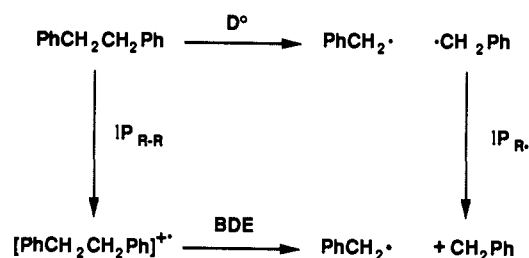
also have a role to play in destroying organic pollutants and hazardous wastes.[19] Radical cations undergo many facile reactions in solution, chief among these are nucleophile addition[5,7-9,20] and deprotonation reactions.[2-9,20-25] Therefore, a thorough un-

(1) (a) This work supported by Gas Research Institute, Basic Coal Science Program, Contract Nos. 5084-260-1087 and 5088-260-1641.

(2) (a) Camaioni, D. M. Effect of Substituents on the Structure and Dissociation Enthalpy of Bibenzyl Radical Cation. Presented at the 22nd Reaction Mechanisms Conference, Pittsburgh, PA, June 13, 1988; poster session 1, paper 8. (b) Camaioni, D. M. Electron Transfer and Radical Cation Reactions of Model Coal Compounds. Final Report to Gas Research Institute, Chicago, IL 60631; GRI Accession Code 88/150; NTIS PB89-102800; Appendix E.

(3) Trahanovsky, W.; Brixius, W. *J. Am. Chem. Soc.* **1973**, *95*, 6778.

(4) Snook, M. E.; Hamilton, G. A. *J. Am. Chem. Soc.* **1974**, *96*, 860.

(5) Walling, C.; Camaioni, D. M.; Kim, S.-S. *J. Am. Chem. Soc.* **1978**, *100*, 4814.

(6) Walling, C.; El-Taliawi, G. M.; Zhao, C. *J. Org. Chem.* **1983**, *48*, 4914.

(7) Camaioni, D. M.; Franz, J. A. *J. Org. Chem.* **1984**, *49*, 1607.

(8) Walling, C.; El-Taliawi, G. M.; Amarnath, K. *J. Am. Chem. Soc.* **1984**, *106*, 7573.

(9) Hammerich, O.; Parker, V. D. *Adv. Phys. Org. Chem.* **1984**, *20*, 141.

(10) Davis, H. F.; Das, P. K.; Reichel, L. W.; Griffin, G. W. *J. Am. Chem. Soc.* **1984**, *106*, 6968.

(11) Okamoto, A.; Snow, M. S.; Arnold, D. R. *Tetrahedron* **1986**, *42*, 6175.

(12) Sankararaman, S.; Perrier, S.; Kochi, J. K. *J. Am. Chem. Soc.* **1989**, *111*, 6448.

(13) Sankararaman, S.; Kochi, J. K. *J. Chem. Soc., Chem. Commun.* **1989**, 1800.

(14) Maslak, P.; Chapman, J., W. H. *J. Chem. Soc., Chem. Commun.* **1989**, 1809.

(15) Maslak, P.; Asel, S. L. *J. Am. Chem. Soc.* **1988**, *110*, 8260.

(16) *Eight Peak Index of Mass Spectra*; Mass Spectrometry Data Center: Reading, U.K. 1974.

(17) Pitt, G. J.; Millward, G. R. *Coal and Modern Coal Processing: An Introduction*; Academic Press: London, 1979.

(18) Schlosberg, R. H. *Chemistry of Coal Conversion*; Plenum Publishing: New York, 1985.

(19) Draper, R. B.; Fox, M. A. *J. Phys. Chem.* **1989**, *93*, 1938–1944.

(20) Schlesener, C. J.; Kochi, J. K. *J. Org. Chem.* **1984**, *49*, 3142.

(21) Sehested, K.; Holcman, J.; Hart, E. J. *J. Phys. Chem.* **1977**, *81*, 1363.

(22) Seshested, K.; Hart, E. J. *J. Phys. Chem.* **1975**, *79*, 1639.

(23) Seshested, K.; Holcman, J. *J. Phys. Chem.* **1978**, *82*, 651.

(24) Schlesener, C. J.; Amatore, C.; Kochi, J. K. *J. Phys. Chem.* **1986**, *90*, 3747.

(25) Baciocchi, E.; Bartoli, D.; Rol, C.; Ruzziconi, R.; Sebastiani, G. V. *J. Org. Chem.* **1986**, *51*, 3587.

derstanding of factors that control radical-cation reactions is necessary for rational development efforts to proceed.

Previously, Camaioni and Franz[7] reported a study of the radical-cation reactions of bibenzyl, the prototypical coal model compound. In this paper, evidence was given that direct cleavage of bibenzyl radical cations with H, Me, or MeO substituents in the 4- and 4'-positions did not compete with deprotonation of the radical cations, whereas C–C scission was the major, if not sole, pathway of reaction if Me and HO substituents were positioned on the ethylene bridge (see Scheme I). These former results were rationalized on the basis that the bibenzyl bond strength is too great to allow bond scission to compete with deprotonation. The effect of substituents in the 4-position on strength of the ethylenic C–C bond was deemed to be small since it was reasoned that electron-donating substituents placed in 4- and 4'-positions would stabilize both the reactant and the cleavage products so that the barrier for scission would be relatively unaffected. Subsequent work by Baciocchi et al.[25] confirmed that bibenzyl radical cation reacts by deprotonation in acetic acid as well as in acetonitrile/water, and Griller et al.[26,27] estimated the bond strength of bibenzyl radical cation to be 22 kcal/mol in acetonitrile. Clearly, the barrier to scission is too high to compete with deprotonation, given that toluene radical cation has a pK_a of -13 in acetonitrile[28] and is deprotonated with a rate constant of 1.0×10^7 s^{-1} in water.[23] To explain the observed cleavage of bicumyl and 1,2-diphenylethanol radical cations, it was reasoned that substituents on the ethylene group would mainly stabilize the products so that the barrier for scission would be reduced, thereby allowing the reaction to be competitive with deprotonation or nucleophilic addition. More recently, rate and thermochemical data have appeared for tri- and tetraphenylethane[29] and p-(dimethylamino)bicumyl[15] radical cations that are supportive of this explanation. However, information on bond strengths of radical cations (ΔH_r°) and on barriers to bond scission ($\Delta H^\ddagger$) is still rather limited.

Bond dissociation energies (BDEs) can be derived from experimental data by use of thermodynamic cycles as demonstrated in Scheme II and eqs 1–4.[26,29,30,33] Gas-phase BDEs are obtained

$$\text{BDE} = \Delta H^\circ_f(R^+) + \Delta H_f^\circ(R^\bullet) - \Delta H^\circ_f(R-R^{\bullet+}) \quad (1)$$

$$= (\Delta H_f^\circ(R^\bullet) + IP(R^\bullet)) + \Delta H_f^\circ(R^\bullet) - (\Delta H_f^\circ(R-R) + IP(R-R)) \quad (2)$$

$$D^\circ = 2\Delta H_f^\circ(R^\bullet) - \Delta H^\circ_f(R-R) \quad (3)$$

$$\text{BDE} = D^\circ + IP(R^\bullet) - IP(R-R) \quad (4)$$

when adiabatic ionization potentials (IP_a) are used in the thermodynamic cycle, and solution-phase BDEs are obtained when redox potentials are used instead of IPs.[26,34] For example, the BDE of bibenzyl radical cation in the gas phase is calculated to be 29 ± 6 kcal/mol by use of recently tabulated thermochemical data for ions and neutral compounds.[35] In an acetonitrile solution, we estimate a value of 24 ± 3 kcal/mol.[36] As pointed out by
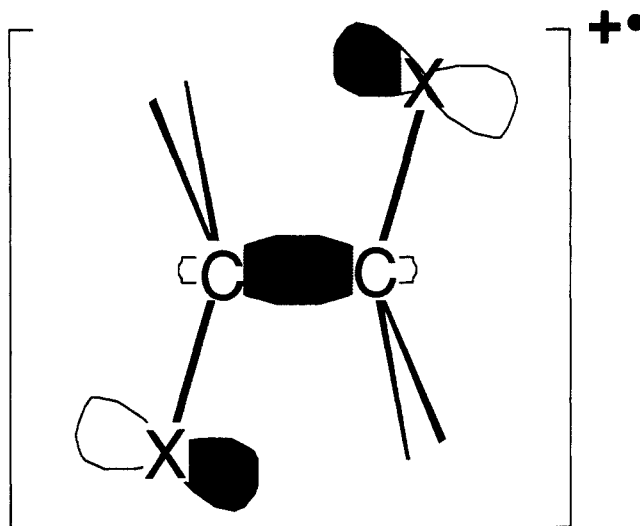

Figure 1. σ/n-Type long-bond structure calculated by Bellville et al.[38] for vicinally substituted ethanes.

Griller et al.,[26] this example shows that gas-phase dissociation energies may be taken as fairly representative of solution-phase values, the exception being those cases where the cationic fragment is much smaller or its charge is more localized causing solvation energies to be very different from that of the radical cation. Even so, structure/reactivity trends discerned from gas-phase data ought to be transferable to the solution phase. Bordwell and Cheng[37] have shown that gas- and solution-phase acidities of cation radicals are linearly correlated.

Overall, the use of thermodynamic cycles for estimating BDEs is limited by the availability and quality of experimental data for radicals and compounds of interest.[26] While a consistent and fairly extensive set of thermochemical data on gas-phase ions and neutral compounds has recently been compiled by Lias et al.,[35] it is by no means all-encompassing. And, because three separate experimental determinations are needed to estimate a radical-cation BDE, errors can accumulate to such an extent that the result is sometimes equivocal. For these reasons, an alternative method for augmenting the experimental data is needed. Calculation by use of molecular orbital (MO) theory is an appealing alternative method. This approach has the benefit of providing structural and electronic information as well as energetics, and it permits inspection of the potential energy surface for dissociation, providing additional insight into the chemical reactivity of radical cations.

Bellville et al.[38] have shown that semiempirical and ab initio MO methods can be coupled to estimate BDEs of vicinally disubstituted ethane radical cations. They used Dewar's semiempirical MNDO method[39] to calculate structures and then computed energies using extended basis set ab initio methods. An interesting outcome of their work[38,40] is that radical cations of alkanes monosubstituted or vicinally disubstituted with HO, NH$_2$, and CHO groups may adopt long-bond "σ/n" structures (see Figure 1) that are substantially lower in energy than n-type structures. However, they predicted that aryl groups would not favor long-bond structures.[38]

The availability of Dewar's improved semiempirical method, AM1,[41] prompted us to explore the ability of AM1 to calculate both radical-cation structures and BDEs while examining more thoroughly the role that through-bond delocalization might play in the reaction chemistry of bibenzylic radical cations. This paper reports our findings, and although it is mainly concerned with dissociation of C–C bonds the approach used here may equally

(26) Griller, D.; Martinho Simoes, J. A.; Sim, B. A.; Wayner, D. D. M. *J. Am. Chem. Soc.* **1989**, *111*, 7872.

(27) Wayner, D. D. M.; Dannenberg, J. J.; Griller, D. *Chem. Phys. Lett.* **1986**, *131*, 3311.

(28) Nicholas, A. M. de P.; Arnold, D. R. *Can. J. Chem.* **1982**, *60*, 2165.

(29) Popielarz, R.; Arnold, D. R. *J. Am. Chem. Soc.* **1990**, *112*, 3068.

(30) Dinnocenzo, J. P.; Todd, W. P.; Simpson, T. R.; Gould, I. R. *J. Am. Chem. Soc.* **1990**, *112*, 2462.

(31) Dinnocenzo, J. P.; Farid, S.; Goodman, J. L.; Gould, I. R.; Todd, W. P.; Mattes, S. L. *J. Am. Chem. Soc.* **1989**, *111*, 8973.

(32) Dinnocenzo, J. P.; Conlon, D. A. *J. Am. Chem. Soc.* **1988**, *110*, 2324.

(33) Ohashi, M.; Akiyama, S. Y. S. *Nippon Kagaku Kaishi* **1989**, 1386.

(34) Although redox potentials are free energies and not enthalpies, the entropy terms for products and reactant may be assumed nearly to cancel out.

(35) Lias, S. G.; Bartmess, J. E.; Liebman, J. F.; Holmes, J. L.; Levin, R. D.; Mallard, W. G. *J. Phys. Chem. Ref. Data* **1988**, *17*, supplement 1.

(36) (a) An $E_{1/2}$ for bibenzyl is not available, but ethylbenzene should be representative: Sasaki, K.; Urata, H.; Uneyama, K.; Nagaura, S. *Electrochim. Acta* **1967**, *12*, 137. Neikam, W. C.; Dimeler, G. R.; Desmond, M. M. *J. Electrochem. Soc.* **1964**, *111*, 1190. (b) $E_{1/2}$ for benzyl: Wayner, D. D. M.; Griller, D. *J. Am. Chem. Soc.* **1985**, *107*, 7764.

(37) Bordwell, F. G.; Cheng, J.-P. *J. Am. Chem. Soc.* **1989**, *111*, 1792.

(38) Bellville, D.; Pabon, R. A.; Bauld, N. L. *J. Am. Chem. Soc.* **1985**, *107*, 4978.

(39) Dewar, M. J. S.; Thiel, W. *J. Am. Chem. Soc.* **1977**, *99*, 4899,4907.

(40) Bellville, D. J.; Bauld, N. L. *J. Am. Chem. Soc.* **1982**, *104*, 5700.

(41) Dewar, M. J. S.; Zoebisch, E. G.; Healy, D. F.; Stewart, J. P. *J. Am. Chem. Soc.* **1985**, *107*, 3902.

Table I. Calculated and Experimental Standard Heats of Formation[a]

formula	name	ΔH_f° (kcal/mol)			formula	name	ΔH_f° (kcal/mol)		
		UHF	RHF	exptl[b]			UHF	RHF	exptl[b]
					Radicals				
CH_3	methyl	30	31.3	34.8 ± 0.3	C_6H_5	phenyl	73.1	79.6	79 ± 1
CH_3O	hydroxymethyl	−27.7	−26.5	−6 ± 1.5	C_6H_5O	phenoxy	4.7	15.7	10 ± 1[d]
CH_4N	aminomethyl	14.3	15.8	38 ± 2	C_7H_7	benzyl	38.6	52	49
C_2H_5	ethyl	15.5	18.2	28 ± 1	C_7H_7O	α-hydroxybenzyl	−10.8	1.3	
C_3H_5	allyl	30.2		39	C_7H_7O	4-hydroxybenzyl	−6.5	7.7	
C_3H_7	isopropyl	3.4	6.7	21 ± 0.5[c]	C_8H_{10}	4-xylyl	30.5	44.7	40
C_4H_9	tert-butyl	−6.4	−2.9	11 ± 0.6	C_9H_{11}	cumyl	20.9	32.9	32 ± 1.4
C_5H_7	pentadienyl	37.7		53	$C_{11}H_9$	1-naphthylmethyl	54		60
					Cations				
CH_3^+	methyl		252.4	261 ± 0.4	$C_7H_7^+$	benzyl		222.1	215 ± 3
CH_3O^+	hydroxymethyl		161.3	168 ± 1.7	$C_7H_7O^+$	α-hydroxybenzyl		161.1	157
CH_4N^+	aminomethyl		175.3	178 ± 5	$C_7H_7O^+$	4-hydroxybenzyl		169.9	153
$C_2H_5^+$	ethyl		216.8	216 ± 1	$C_8H_9^+$	1-phenylethyl		206.5	199
$C_2H_5O^+$	hydroxyethyl		140.7	139 ± 2	$C_8H_9^+$	4-xylyl		209.9	200 ± 3
$C_3H_5^+$	allyl		226.2	226 ± 0.5	$C_8H_9O^+$	α-hydroxy-4-xylyl		150.3	144
$C_3H_7^+$	isopropyl		191.9	190 ± 1	$C_8H_9O^+$	1-hydroxy-1-phenylethyl		149.1	140
$C_3H_7O^+$	2-hydroxypropyl		125.5	117	$C_8H_9O_2^+$	1-hydroxy-1-(4-anisyl)-ethyl		115.8	104
$C_4H_9^+$	tert-butyl		173.9	166 ± 1.3					
$C_4H_9O^+$	2-hydroxybutyl		117.2	109	$C_9H_{11}^+$	cumyl		194.4	186
$C_5H_7^+$	pentadienyl		222.6	220	$C_{11}H_9^+$	1-naphthylmethyl		233.0	229
					Radical Cations				
CH_4^+	methane	274.3		271 ± 1.3	$C_8H_{10}O^+$	ethyl phenyl ether	167.1		163 ± 0.6
$C_2H_6^+$	ethane	236.8	237.1[e]	245.6 ± 0.3	$C_9H_{12}^+$	n-propylbenzene, ⊥[f]	202.1	205.8	203 ± 0.4
$C_2H_6O^+$	ethanol	173.4		185.3 ± 0.6	$C_9H_{12}^+$	n-propylbenzene, ‖	203.1	206.9	
$C_2H_6O_2^+$	ethylene glycol	114.4	114.8	142 ± 2	$C_{10}H_{14}^+$	isobutylbenzene, ⊥	199.1	203.0	195 ± 0.5
$C_2H_7N^+$	ethylamine	181.5		193 ± 0.7	$C_{10}H_{14}^+$	isobutylbenzene, ‖	200.2	203.9	
$C_2H_7NO^+$	ethanolamine	139.7		158 ± 2	$C_{11}H_{16}^+$	neopentylbenzene, ⊥	195.3	199.4	187
$C_2H_8N_2^+$	ethylenediamine	171.1	173.4	194 ± 5	$C_{13}H_{12}^+$	diphenylmethane	241.1	249.1	230 ± 1.4
$C_3H_8^+$	propane	219.7		227 ± 1.25	$C_{13}H_{12}O^+$	benzyl phenyl ether	215.0	224.3	
$C_4H_{10}^+$	butane	211.3		213 ± 2.4	$C_{14}H_{14}^+$	bibenzyl, ‖	234.9	244.7[e]	235 ± 2.7
$C_5H_{12}^+$	pentane	202.5		204 ± 03	$C_{14}H_{14}^+$	bibenzyl, ⊥	235.5	241.8[e]	
$C_6H_6^+$	benzene	231.5		233.2 ± 0.1	$C_{14}H_{14}O_2^+$	1,2-dihydroxy-1,2-diphenylethane	151.4	156.7	
$C_6H_6O^+$	phenol	173.1		173 ± 1.35					
$C_6H_{14}^+$	2,3-dimethylbutane	183.8		189 ± 1.25	$C_{14}H_{14}O^+$	1,2-diphenylethanol	190.4	198.4	
$C_7H_8^+$	toluene	215.9		215 ± 0.3	$C_{14}H_{14}O_2^+$	4,4'-dihydroxybibenzyl	136.1	144.2	
$C_7H_8O^+$	anisole	174.9		173 ± 0.8	$C_{16}H_{18}^+$	1,2-di-4-tolylethane	213.6	227.1	
$C_7H_8O^+$	benzyl alcohol	173.5		172	$C_{18}H_{24}$	bicumyl	232.6	239.7[e]	
$C_7H_8O^+$	4-cresol	160.3		157 ± 1.7					
$C_8H_{10}^+$	ethylbenzene, ‖[f]	209.3	212.9	209 ± 0.3					

[a] Calculated values obtained by use of AM1 (AMPAC, QCPE No. 506); UHF values are geometry optimized; RHF values are calculated with UHF-optimized geometries unless noted. [b] Experimental values from Lias et al.,[35] unless noted. [b] Error limits for experimental values are ±5 kcal/mol for cationic species and ±2 kcal/mol for radicals unless noted. [c] Back.[42] [d] Tschuikow-Roux and Chen.[42] [e] RHF geometry optimized value. [f] ‖ and ⊥ designate conformations of Ar-CH₂-R radical cations where R is, respectively, in the plane or perpendicular to the plane of the aryl ring bearing the positive charge.

well be applied to bonds between heteroatoms.

Methodology

AM1 calculations were performed on a MicroVAX (Digital Equipment Corp., Maynard, MA) computer with AMPAC (Quantum Chemistry Program Exchange, Department of Chemistry, Indiana University, Bloomington, IN; QCPE No. 506). Geometries of radical cations and their cation and radical fragmentation products were optimized by use of the unrestricted Hartree–Fock (UHF) Hamiltonian. Restricted Hartree–Fock (RHF) energies were obtained for UHF geometries from single-point calculations. RHF calculations include half-electron configuration interaction (CI) for radicals and radical cations. Test calculations for radical cations of ethane, ethylbenzene, bibenzyl, and bicumyl showed that this approach gives results comparable to full optimization in the RHF potential energy space and provides a significant advantage over performing geometry optimizations in RHF-CI potential energy space in that calculation times are much shorter. UHF and RHF geometries typically differed at most by one digit in the fourth significant figure for bond distances and the third significant figure for bond angles and dihedral angles. Energies of structures optimized with the RHF Hamiltonian differed by less than 1 kcal/mol from energies obtained by single-point RHF calculations with use of geometries optimized with the UHF Hamiltonian.

Reaction paths for C–C bond scission were computed with the reaction-coordinate option in AMPAC. The method fixs the C–C bond distance and optimizes the other internal coordinates (bond distances, angles, and dihedral angles) to find a minimum energy structure for each of a series of specified bond distances. Potential energy maxima corresponding to transition states (TS) for exothermic bond dissociations were each determined by fitting to a quadratic equation three points that bracketed the maximum, solving the first derivative of the quadratic equation to obtain the C1–C2 bond distance for the TS structure, and in turn using

this number to solve for the energy of the maximum (TS) of the quadratic equation.

Experimental values were obtained from thermochemical data found in the literature.[35,42,43] Unless otherwise indicated, errors in heats of formation (ΔH°_f) of cations and radical cations are estimated to be ±5 kcal/mol[35] and errors in ΔH_f° of radicals are estimated to be ±2 kcal/mol.[43]

Molecular orbital density plots were generated from AM1 geometries with Version 3.6 of the Quantum Chemistry Interactive Program Utility (QUIPU) supplied by the Florida School on Applied Molecular Orbital Theory (Quantum Theory Project, Departments of Chemistry and Physics, University of Florida, Gainesville, FL). Screen images of MO plots were captured from a Macintosh SE (Apple Computer, Inc., Cupertino, CA) screen by use of MAC240 terminal emulation software (Whitepine Software, Inc., Amherst, NH) and were redrawn for clarity with MACDRAW II (Claris Corp., Mountain View, CA).

Results and Discussion

BDEs. Table I provides calculated and experimental ΔH_f° for a wide variety of organic radical cations, with results of both UHF and RHF calculations being provided for comparison. Table II lists calculated and experimental BDEs for several radical cations, and Table III compares these radical-cation BDEs with homolytic BDEs (D°) for the neutral compounds. It is interesting to note the degree to which bond energies are lowered by ionizing a neutral compound to a radical cation. The reduction is substantial for

(42) (a) D° for homolytic scission of bicumyl: Kratt, G.; Beckhaus, H.-D., Ruchardt, C. *Chem. Ber.* **1984**, *117*, 1748. (b) ΔH°_f(phenoxyl): Back, M. H. *J. Phys. Chem.* **1989**, *93*, 6880. (c) ΔH°_f(isopropyl): Tschuikow-Roux, E.; Chen, Y. *J. Am. Chem. Soc.* **1989**, *111*, 9030.

(43) Benson, S. W. *Thermochemical Kinetics*; Wiley: New York, 1976.

Table II. Calculated and Experimental Bond Dissociation Energies[a]

radical cation	R1[+]	R2[·]	BDE (kcal/mol)		
			UHF	RHF	exptl
		Aliphatic			
ethane	Me	Me	46	47	50 ± 1
butane	Et	Et	21		31 ± 4
2,3-dimethylbutane	i-Pr	i-Pr	12		23 ± 3
ethylamine	H₂NCH₂	Me	24		20 ± 6
ethanol	HOCH₂	Me	18		18 ± 3
ethanolamine	H₂NCH₂	CH₂OH	8		14 ± 9
ethylenediamine	H₂NCH₂	CH₂NH₂	19	18	22 ± 12
ethylene glycol	HOCH₂	CH₂OH	19	20	20 ± 5
		Aromatic			
diphenylmethane	PhCH₂	Ph	54	53	64 ± 5
ethylbenzene	PhCH₂	Me	43	41	41 ± 4
n-propylbenzene	PhCH₂	Et	36	35	40 ± 4
isobutylbenzene	PhCH₂	i-Pr	26	26	41 ± 4
neopentylbenzene	t-Bu	CH₂Ph	17	27	28 ± 1
bibenzyl	PhCH₂	CH₂Ph	26	32	29 ± 6
1,2-di-4-tolylethane	MePhCH₂	CH₂PhMe	27	28	
4,4'-dihydroxybibenzyl	HOPhCH₂	CH₂PhOH	27	33	
1,2-diphenylethanol	PhCHOH	CH₂Ph	9	15	
stilbene glycol	HOPhCH₂	CH₂PhOH	−1	6	
bicumyl	PhCMe₂	PhCMe₂	−17	−12	
ethyl phenyl ether	Et	OPh	54		63 ± 1
benzyl phenyl ether	PhCH₂	OPh	12	14	

[a] From data in Table I.

Table III. Comparison of Radical-Cation and Homolytic Bond Dissociation Energies

radical cation	R1	R2	BDE (kcal/mol)	
			radical cation	neutral
diphenylmethane	PhCH₂	Ph	64	95
ethylbenzene	PhCH₂	Me	41	77
n-propylbenzene	PhCH₂	Et	40	75
isobutylbenzene	PhCH₂	i-Pr	35	76
neopentylbenzene	t-Bu	PhCH₂	21	73
ethane	Me	Me	51	90
ethylene glycol	HOCH₂	HOCH₂	20	80
ethylenediamine	CH₂NH₂	CH₂NH₂	22	80
bibenzyl	PhCH₂	PhCH₂	29	64
benzyl phenyl ether	PhCH₂	PhO	12[b]	53[c]
4,4'-dihydroxybibenzyl	HOPhCH₂	HOPhCH₂	(26)[b,d]	64[c]
1,2-diphenylethanol	PhCHOH	PhCH₂	(14)[b,d]	58[c]
stilbene glycol	PhCHOH	CHOHPh	(11)	52[c]
bicumyl	PhCMe₂	PhCMe₂	(−10)	46[e]

[a] Radical-cation BDEs are for cationic R1 fragment. Values are from experimental data[35] except as noted. [b] Uses corrected AM1 $\Delta H°_f$(radical cation); see Tables I and IV. [c] Uses $\Delta H°_f$(neutral) estimated by group additivity methods.[43] [d] Uses corrected AM1 $\Delta H°_f$ (radical); see Tables I and IV. [e] Kratt et al.[42]

these radical cations; some BDEs are even predicted to be negative.

Comparison of the experimental and calculated radical-cation BDEs in Table II shows that AM1 generally yields BDEs that are smaller than experimentally derived values. Overall, the agreement with experimental BDEs is much better than might be expected considering the range of disagreement between the calculated and experimental $\Delta H°_f$. Yet, a uniform difference or systematic relationship between the experimental and calculated BDEs is not evident. Thus, the sometimes large differences (e.g., diphenylmethane, isobutylbenzene, neopentylbenzene, ethyl phenyl ether, ethanolamine, n-butane, and dimethylbutane) that are encountered between experiment and theory raise concern about the use of AM1 to predict BDEs.

Both MNDO and AM1 have been noted to give large errors in $\Delta H_f°$ for organic nitro compounds; however, the errors were found to be systematic such that corrections could be applied.[44,45] Recently, an analysis by Kass[46] of AM1-calculated hydrocarbon
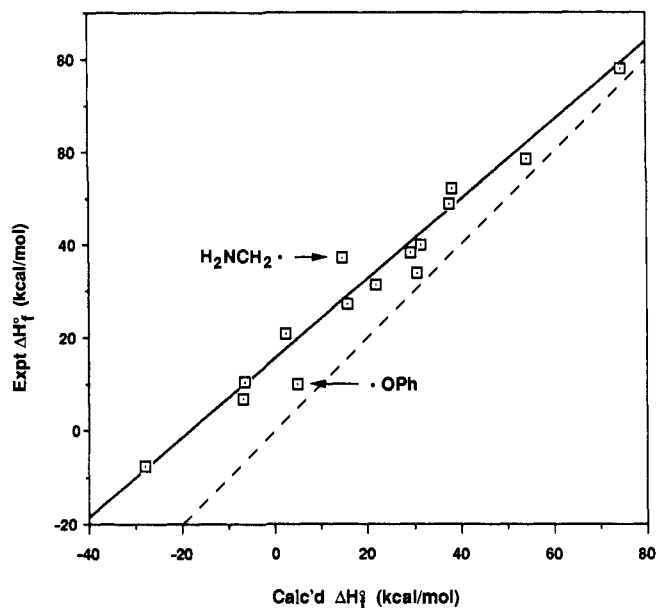
(44) Davis, L. P.; Storch, D. M.; Guidry, R. M. *J. Energ. Mater.* **1987**, 5, 89.

(45) Stewart, J. J. P. *J. Comput. Chem.* **1989**, 10, 221.

Figure 2. Linear correlation of experimental vs calculated (UHF) $\Delta H_f°$ for radicals in Table I. Dotted line represents correlation that would pertain if agreement between experiment and calculation were exact.

acidities showed that errors in anion $\Delta H°_f$ were systematic and that an empirical correction could be applied on the basis of a linear correlation obtained for experimental and calculated anion values. Data in Table I also were subjected to regression analysis, and analogous linear correlations were found to exist for radicals, cations, and radical cations.

Figures 2–4 show plots of experimental and calculated $\Delta H_f°$, and Table IV lists linear regression parameters for trial correlations. Standard deviations in UHF correlations are about 4 kcal/mol for aromatic radical cations and about 5 kcal/mol for ethane radical cations. These values are larger than many of the uncertainties in Table I, but comparable to uncertainties in much of the experimental data compiled by Lias et al.[35] The standard deviation in the UHF radical data is also about 5 kcal/mol. This is more than twice the uncertainties typically associated with radical $\Delta H_f°$.[43] Inspection of the plot for radicals indicates that

(46) Kass, S. R. *J. Comput. Chem.* **1990**, 11, 94–104.

Through-Bond Delocalization in Bibenzylic Systems

J. Am. Chem. Soc., Vol. 112, No. 26, 1990 9479
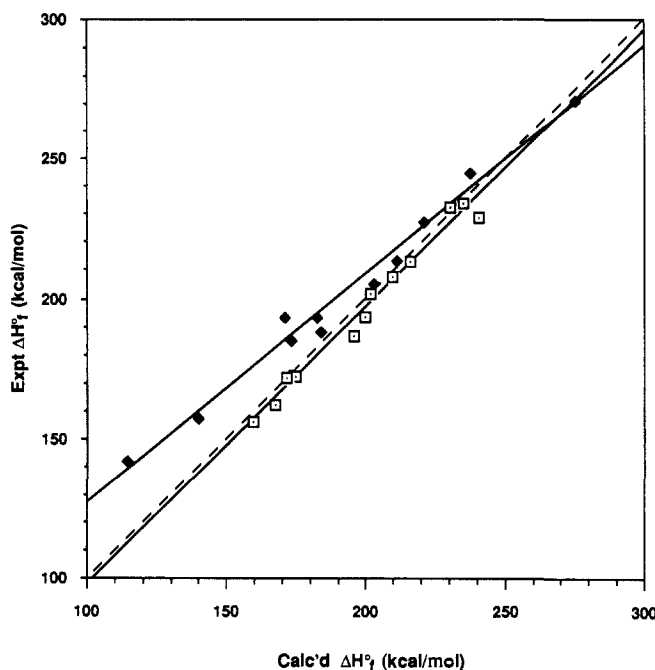
Figure 3. Linear correlations of experimental vs calculated (UHF) ΔH_f° for radical cations in Table I: ($\blacklozenge$) aliphatic radical cations; ($\square$) aromatic radical cations. Dotted line represents correlation that would pertain if agreement between experiment and calculation were exact.

Table IV. Linear Regression Results for Correlations of Experimental vs Calculated ΔH°_f

type	method	no. of pts	slope	intercept	variance[a]	correln coeff
all	RHF	41	0.94	7.9	93	0.993
radicals + radical cations	UHF	38	0.94	15	56	0.992
radicals	UHF	14	0.84	16	23	0.978
radicals[b]	UHF	12	0.83	16	9	0.992
radicals	RHF	11	0.74	13	56	0.949
arene radical cations	UHF	13	0.99	-1.0	15	0.991
ethane radical cations	UHF	11	0.82	45	29	0.990
arene radical cations	RHF	9	0.72	57	110	0.948
cations	RHF	21	1.06	-16	33	0.992
alkyl cations	RHF	4	1.19	-41	4.1	0.999
benzylic cations	RHF	8	1.22	-54	6.4	0.996
α-hydroxyalkyl cations	RHF	4	1.36	-52	3	0.999
α-hydroxybenzylic cations	RHF	4	1.16	-30	2.9	0.998

[a] Square of the standard deviation in y. [b] Phenoxy and aminomethyl radicals excluded from fit.

much of the standard deviation is associated with the inclusion of aminomethyl and phenoxy radicals. If these two data are excluded on the basis that these radicals are outside the data set that consists mainly of carbon-centered radicals, then the standard deviation in predicted ΔH_f° improves to about 3 kcal/mol, which approaches the real errors associated with experimental data. The correlation for cations gives a standard deviation of about 6 kcal/mol. However, significantly better correlations are obtained by dividing the cations into subclasses: alkyl, allylic/benzylic, α-hydroxyalkyl, α-hydroxybenzylic. Standard deviations (1.7–2.5 kcal/mol) obtained for these correlations are well within the experimental error associated with much of the cation data. Correlations of RHF-calculated ΔH_f° values for radicals and radical cations provide results similar to correlations of the UHF data, although larger standard deviations in predicted ΔH_f° are obtained as a consequence of having smaller data sets (see Table IV).

This analysis shows that the differences observed between AM1 and experimental ΔH_f° are systematic and not random, as might
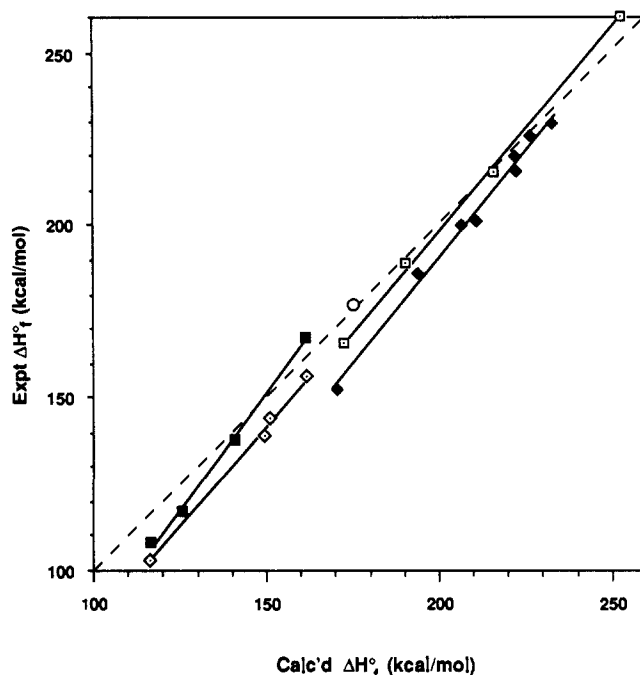

Figure 4. Linear correlations of experimental vs calculated ΔH_f° for cations in Table I: ($\square$) alkyl; ($\blacklozenge$) allylic/benzylic; ($\blacksquare$) hydroxyalkyl; ($\lozenge$) 1-hydroxy-1-phenylalkyl; (O) aminomethyl. Dotted line represents correlation that would pertain if agreement between experiment and calculation were exact.
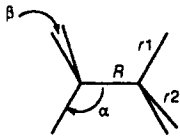
be construed from a cursory look at the data in Table I, and furthermore, it provides a key for relating calculated ΔH_f° to experimental values. The variability between calculated and experimental ΔH_f° is now understood to be due to correlations having nonunit slopes and nonzero intercepts that differ according to the chemical class/species to which a compound belongs. From Figures 2–4, it can be seen that how well a compound's calculated ΔH_f° agrees with experiment depends on how different its correlation's slope and intercept are from unity and zero and how near its ΔH_f° is to the point where the line represented by a slope of 1 and intercept of 0 (dotted lines in Figures 2–4) crosses the line representing its correlation.

In view of how different the correlations are for the species considered here, it is now understandable that the differences between calculated and experimental BDEs vary so much. They are obtained by combining ΔH_f° values from three different compound classes. Furthermore, it should be understood from this analysis that even when a reaction is a simple isomerization such that reactant and product are structurally related, if the slope of the correlation between experiment and calculated is not unity then although the offsets may be canceled in subtracting two ΔH_f°, the resulting ΔH_r° will be in error by a factor equal to the slope of the correlation. Clearly, quantative knowledge such as that provided by the analysis in Table IV is vital to using AM1 theory as a predictive tool.

The above findings suggest that AM1 can be used to estimate heats with accuracies that may approach that of an experimental value. Several of the radical-cation bond dissociation reactions in Table III involve species for which there are no experimental data available. Accordingly, we estimated their BDEs using AM1-calculated ΔH_f° corrected with the appropriate correlation in Table IV. These BDEs are shown within parentheses in Table III.

Correlating AM1 ΔH_f° with experimental values can also help resolve conflicts in the literature. For example, two very different ΔH_f° for p-hydroxybenzyl cation are included in the recent tabulation of ion thermochemistry by Lias et al:[35] 153 and 175 kcal/mol.[47] The latter value derived from appearance potential

(47) Russell, D. H.; Freiser, B. S.; McBay, E. H.; Canada, D. C. *Org. Mass Spectrom.* **1983**, *18*, 474.

9480 *J. Am. Chem. Soc., Vol. 112, No. 26, 1990*

Camaioni

Table V. Comparison of AM1 and ab Initio Calculations for Ethane Radical Cation[a]

state	ΔE	structural parameters				
		R	$r1$	$r2$	α	β
		AM1[b]				
$^2B_g(C_{2h})$	-1	1.428	1.117	1.167	116.0	89.5
$^2A_g(C_{2h})$	0^c	1.439	1.200	1.126	101.5	113.7
$^2A_{1g}(D_{3d})$	14	2.046	1.104	1.104	96.4	118.7
		Ab Initio[d]				
$^2A_g(C_{2h})$	0^e	1.579	1.131	1.081	82.6	115.8
$^2A_{1g}(D_{3d})$	3.8	1.918	1.082		98.3	

[a] Energies in kilocalories per mole, distances in angstroms, and angles in degrees. R, $r1$, and α are for in-plane H-C-C-H; $r2$ and β are for out-of-plane H-C-H. [b] Geometry-optimized RHF calculations. [c] $\Delta H°_f = 238.0$ kcal/mol. [d] MP2/6-31G**,[50] [e] Total energy = $-79.131\ 290$ hartrees (1 hartree = 627.51 kcal/mol).

measurements is given preferential listing. However, the former value, determined by proton affinity measurements on 4-methylene-2,5-cyclohexadien-1-one better correlates with AM1 values for benzylic/allyic cations, suggesting it is the more accurate value.

Structures of Radical Cations. AM1 finds geometries for radical cations that are qualitatively similar to structures found by ab initio[48-50] and experimental methods.[15,51-56] For example, AM1 locates three energy minima for ethane radical cation with $\Delta H_f°$ of 237.1, 238.1, and 252.2 kcal/mol (see Table V). The two lower states have C_{2h} symmetry, and the highest state has D_{3d} symmetry. The structures with C_{2h} symmetry are consistent with the ^2B_g and ^2A_g states described by Richartz et al.[48] for ionization out of the doubly degenerate $1e_g$ MO of neutral ethane. These structures exhibit the expected Jahn-Teller distortions in which the C-C bond distances are shortened and the bond angles are distorted relative to ethane. For the ^2B_g structure, the H-C-H angle between out-of-plane hydrogens is 89.5° and the H-C-C angles for in-plane and out-of-plane hydrogens are 113 and 116°, respectively. The ^2A_g state adopts a "diborane-like" structure with H-C-C angles for in-plane hydrogens being 99.6° and H-C-H angles 113.7°. The highest of the three energy minima has D_{3d} symmetry with bond length and bond angle distortions consistent with the $^2A_{1g}$ state formed by ionization out of the $3a_{1g}$ MO of ethane. The C-C bond is elongated relative to ethane, and the bond angles are changed such that the methyl groups are in between tetrahedral and planar values.

Ab initio computations[48-50] for ethane radical cation have found similar structures. Calculations by Richartz et al.[48] found both ^2A_g and $^2A_{1g}$ states to be lower than the ^2B_g state while calculations by Bouma et al.[49] found the $^2A_{1g}$ state to be the global minimum. Bouma[49] found the ^2B_g state to be as little as 3-7 kcal/mol higher in energy depending on the basis set and level of electron correlation incorporated in the calculation (the energy difference between the two states is smallest for calculations using Møller-Plesset perturbation theory[57,58] terminated at the second order with
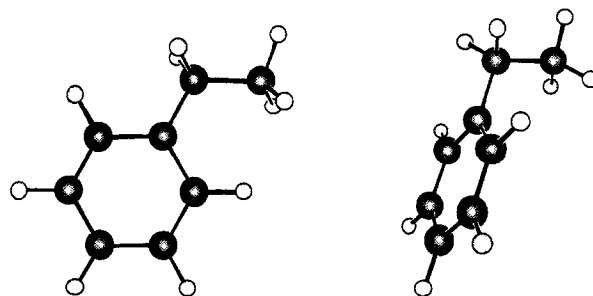
$\Delta H°_f = 109$ kcal/mol $\Delta H°_f = 110$ kcal/mol

Figure 5. Conformations and energies (kcal/mol) calculated for ethylbenzene radical cation. The favored conformation has the ethyl group in the plane of the aromatic ring. Charge in both structures is mainly at ipso and para positions.

A   B

UHF: $\Delta H°_f = 234.8$ UHF: $\Delta H°_f = 235.5$
RHF: $\Delta H°_f = 244.7$ RHF: $\Delta H°_f = 241.8$
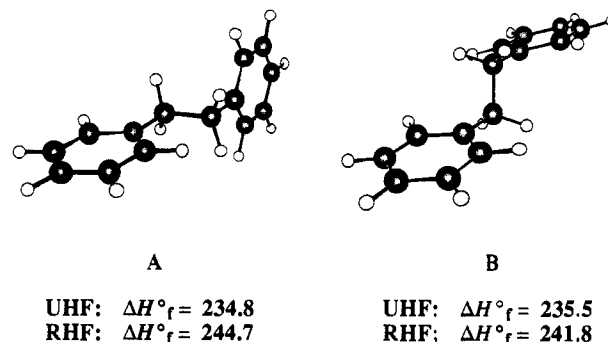
Figure 6. Conformations and energies (kcal/mol) calculated for bibenzyl radical cation. Charge is mainly delocalized in the ring shown in the foreground.

a 6-31G* basis set[59]). They did not find a minimum for the ^2A_g state. More recently, ab initio calculation by Lunell and Huang[50] took Bouma's calculations[49] to higher sophistication by including polarization functions on both carbon and hydrogen and found that the ^2A_g state is 3.8 kcal/mol lower than the $^2A_{1g}$ state. The calculated structure of the ^2A_g state is "diborane-like" (C_{2h} symmetry with in-plane hydrogens that have a H-C-C bond angle of 82.6° and C-C distance of 1.579 Å). this structure is qualitatively very similar to the second lowest state, ^2A_g, calculated by AM1 (see Table V). This structure also appears to be most consistent with the electron spin resonance (ESR) spectrum of Toriyama et al.,[51] showing two equivalent hydrogens with a large 152.5-G coupling constant. Lunell and Huang[50] did not report on the ^2B_g state. Thus, how the ^2B_g state is affected by polarization functions on the hydrogens is not known. AM1 apparently does not agree with ab initio calculations or ESR results as to the ordering of states for ethane radical cation; however, it does find structures consistent with the range of possibilities, and it does so with a minimum of effort. Thus, AM1 structures ought to be good starting points for ab initio calculations.

Bouma et al.[49] calculated an ab initio BDE for ethane radical cation of 45 kcal/mol that compares very well with AM1's value of 45.5.[60]

AM1 results for the radical cations of ethylbenzene and diarylethanes are consistent with experimental structures deduced from experiment.[15,51-53] AM1 finds two conformations for ethylbenzene radical cation. The lower energy conformation is

(48) Richartz, A.; Buenker, R. J.; Bruna, P. J.; Peryimhoff, S. D. *Mol. Phys.* **1977**, *33*, 1345.

(49) Bouma, W. H. Poppinger, D.; Radom, L. *Isr. J. Chem.* **1983**, *23*, 21.

(50) Lunell, S.; Huang, M.-B. *J. Chem. Soc., Chem. Commun.* **1989**, 1031.

(51) Toriyama, K.; Nunome, K.; Iwasaki, M. *J. Chem. Phys.* **1982**, *77*, 5891.

(52) Rao, D. N. R.; Symons, M. C. R. *J. Chem. Soc., Perkin Trans. 2* **1985**, 991.

(53) Tehara, A.; Ohya-Nishiguchi, H.; Hirota, N.; Higuchi, H.; Misumi, S. *J. Phys. Chem.* **1986**, *90*, 4958.

(54) Delcourt, M. O.; Rossi, J. J. *J. Phys. Chem.* **1982**, *86*, 3234.

(55) Badger, B.; Brocklehurst, B. *Trans. Faraday Soc.* **1969**, *65*, 2582.

(56) Irie, S.; Horii, H.; Irie, M. *Macromolecules* **1980**, *13*, 1355.

(57) Møller, C.; Plesset, M. S. *Phys. Rev.* **1934**, *46*, 618.

(58) Pople, J. A.; Binkley, J. S.; Seeger, R. *Int. J. Quantum Chem., Symp.* **1976**, *10*, 1.

(59) Hariharan, P. C.; Pople, J. A. *Theor. Chim. Acta* **1973**, *38*, 213.

(60) (a) A downward correction of up to 2.4 kcal/mol may be necessary since AM1 energies are enthalpies at 300 °C whereas ab initio values are total energies at 0 K. (b) Cottrell, T. L. *The Strength of Chemical Bonds*; Butterworths: London, 1958. (c) Cox, J. D.; Pilcher, G. *Thermochemistry of Organic and Organometallic Compounds*; Academic Press: New York, 1979; pp 516.
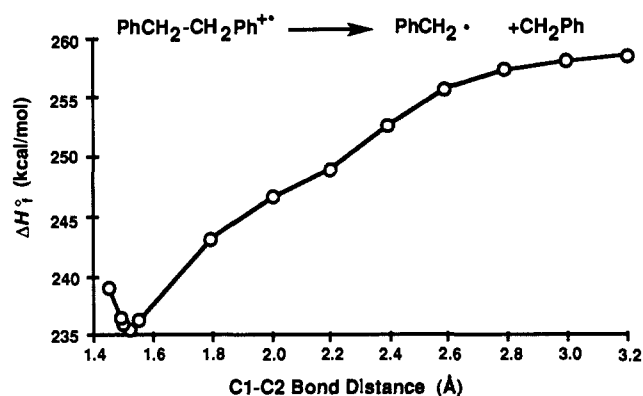
Through-Bond Delocalization in Bibenzylic Systems

J. Am. Chem. Soc., Vol. 112, No. 26, 1990 9481

Figure 7. UHF potential energy diagram for dissociation of bibenzyl cation. Stretching the C–C bond allows the structure to adopt conformation B (Figure 3) and enables through-bond delocalization between both phenyl groups. A symmetrical structure (C_{2h}) occurs at 2.1 Å. No evidence was found for through-space resonance interactions between the rings.

the one with the ethyl group in the plane of the benzene ring (see Figure 5). The same conformation is observed by Rao and Symons[52,61] in a Freon matrix at 77 K. AM1 indicates that bibenzylic cations are π-type structures with charge mainly localized in just one of the aromatic rings, as predicted by Bellville et al.[38] and consistent with ESR data for a series of bicumyl radical cations[15] and for the bibenzyl analogue 1,2-di-9-anthrylethane radical cation.[53] Conformations exhibiting through-space interactions between the phenyl rings of bibenzylic radical cations are not favored by AM1. Interestingly, UHF and RHF methods differ on the minimum energy conformation of bibenzyl radical cation (see Figure 6). The UHF potential energy surface favors a conformation that has the ethylene group in the plane of the ring bearing the positive charge as with ethylbenzene radical cation such that hyperconjugation with the aliphatic hydrogens is maximized. The RHF potential energy surface favors a conformation that has the ethylene group perpendicular to the ring bearing the positive charge such that hyperconjugation with the C–C bond is maximized. No ESR spectra of bibenzyl radical cation are available to indicate which of these results is more consistent; however, the conformation favored by UHF is similar to the structure deduced by ESR for the analogous 1,2-di-9-anthrylethane radical cation.[53] This radical cation adopts a conformation having the ethylenic C–C bond 28° out of the plane of the charge-bearing anthracene ring. This conformation is most like conformer A for bibenzyl radical cation in Figure 6. It has an out-of-plane angle of 5°. The result suggests that, in absence of steric interactions with peri hydrogens, a conformation with ethylenic bond coplanar with the anthracene ring would be preferred for dianthrylethane radical cation. Electronic spectra of bibenzyl radical cation in solution[54] and in solid matrices[55,56] are reported to show charge resonance bands that have been attributed to through-space interactions. Through-bond interactions in a conformation such as that favored by RHF calculations (see structure B in Figure 6) could possibly accommodate these observations.

As in the MNDO calculations of Bellville et al.,[38] our calculations with AM1 find long-bond minima for ethylene glycol and ethylenediamine radical cations (C–C bond lengths are, respectively, 2.11 and 2.17 Å). Long-bond minima in the UHF potential energy surface are also found for ethanolamine and 2,3-dimethylbutane radical cations. Ethanol and ethylamine radical cations are predicted to have long-bond minima, too, but structures with normal bond lengths are predicted to have minima that are lower in energy. To our knowledge, no long-bond structures for any of these compounds have been confirmed experimentally.

Reaction-Coordinate Calculations for C–C Cleavage. The reaction paths for C–C bond scission of bibenzylic radical cations
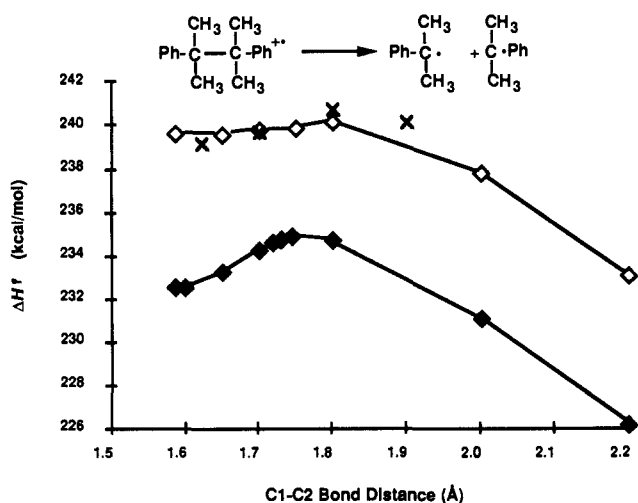
(61) Rao, D. N. R.; Chandra, H.; Symons, M. C. R. *J. Chem. Soc., Perkins Trans. 2* **1984**, 1201.

Figure 8. Reaction-coordinate diagram calculated for dissociation of bicumyl cation: (◇) RHF values for UHF-optimized geometry; (◆) geometry-optimized UHF values; (×) geometry-optimized RHF values. The transition state for C–C bond cleavage is achieved at 1.75 Å with a barrier height of 2.3 kcal/mol on the UHF surface. RHF calculations predict a later TS at 1.81 Å with a smaller barrier of 1.6 kcal/mol and a less exothermic scission.
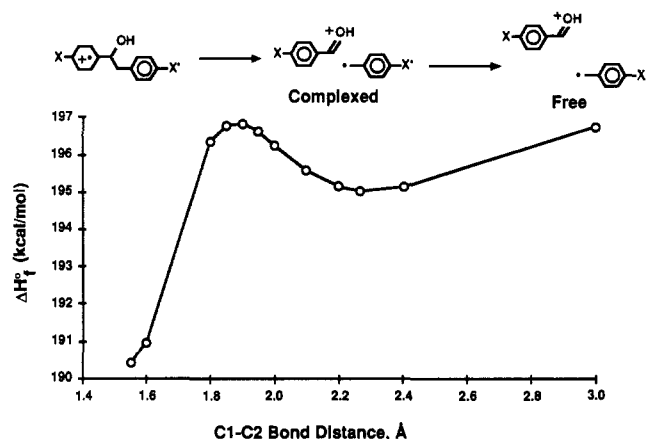

Figure 9. UHF potential energy diagram calculated for dissociation of 1,2-diphenylethanol cation. The long-bond structure appears to be a loosely bound complex between benzyl radical and α-hydroxybenzyl cation.

were also investigated (see Methodology). The calculations suggest that stretching the central C–C bond enables delocalization into the β-substituents through the C1–C2 bond (see Figures 7–10). Through-bond delocalization is well-established in bibenzyl radical cation for bond lengths of 1.8–2.4 Å, but at a cost of >10 kcal/mol energy (see Figure 7). A structure with C_{2h} symmetry is achieved for bibenzyl radical cation at a C1–C2 bond distance of 2.1 Å in the UHF potential energy space (no symmetry contraints were imposed). Charge is symmetrically distributed in this structure over both phenyl groups through the C1–C2 bond.

Neither methyl nor hydroxyl substituents on the phenyl rings are calculated to stabilize the long-bond structure enough to cause it to become a minimum in either the UHF or RHF potential energy surface. However, their substitution on the ethylene group is calculated to change substantially the potential energy surface for bond scission (see Figures 8 and 9).

Reaction-path calculations for bicumyl radical cation are interesting because bond scission is calculated to be exothermic and saddle points are traversed on the way to products (Figure 8). Of interest here is the barrier height and the structure of the of TS. The reaction path for bicumyl radical cation was investigated in both UHF and RHF potential energy space. Both single-point RHF calculations with use of UHF geometries and geometry-optimized RHF calculations were performed and found to provide comparable results. The UHF and RHF potential energy surfaces

9482   *J. Am. Chem. Soc., Vol. 112, No. 26, 1990*

Camaioni
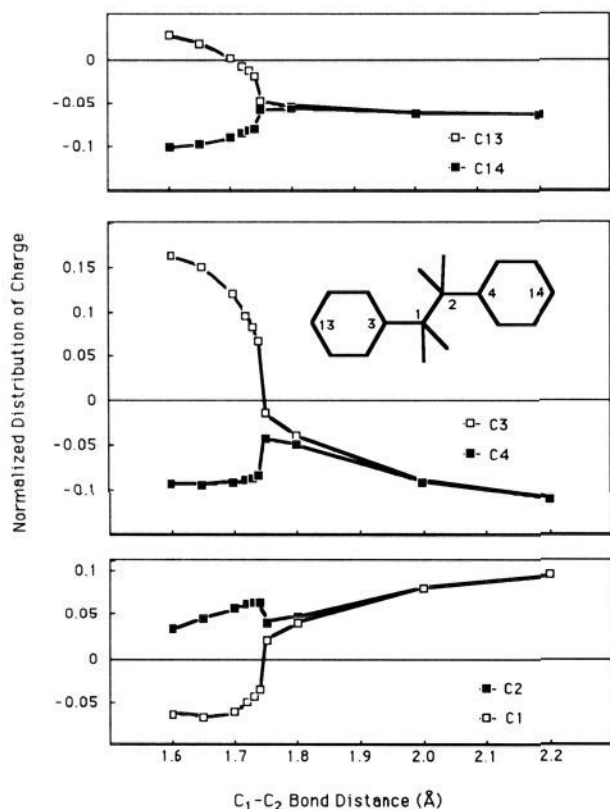
Figure 10. Distribution of charge in bicumyl radical cation as a function of the C1–C2 bond. Formal charges are from UHF calculations normalized to +1. The TS is attained at 1.75 Å.

differ in that the barrier to dissociation is lower and the TS is later on the RHF surface. The TS for cleavage of the bicumyl C–C bond is achieved at ~1.75 with a barrier height of 2.3 kcal/mol on the UHF potential energy surface compared to ~1.81 Å with a barrier of 1.6 kcal/mol on the RHF surface.

Figure 10 shows how calculated formal charge redistributes in bicumyl cation as the C1–C2 bond is lengthened from 1.6 to 2.2 Å. Elongating the C1–C2 bond brings about an equalization of electron density between the halves of the structure. Prior to the TS, C1, C3, and C13 are electron deficient relative to C4 and C14. At the TS (1.74–1.75 Å), electron density at these atoms is nearly equalized, with C1 and C2 being deficient in electron density relative to the other atoms. After the TS, the deficiency at C1 and C2 further increases while it decreases at C3 and C4. These trends are consistent with the phenyl π-systems becoming delocalized through the central C–C bond in the TS. Note that substantial delocalization occurs even though C1 and C2 of the TS structure are pyramidal and a good deal closer to sp³ hybridization than sp² hybridization. The C1–C2–C3 and C2–C1–C4 bond angles that correspond to the angle between the plane of each benzene ring and the C1–C2 bond decrease continuously as the bond is stretched. These angles are tetrahedral in the reactant geometry and differ by about 1° until TS is reached, at which point they are very nearly equal at 105°. At 2.2 Å, values are calculated to be 100°. Values of 90° correspond to free cumyl radical and cumyl cation.

To establish more clearly that through-bond delocalization accounts for these findings, the spatial distributions of the singly occupied molecular orbital (SOMO) of the bicumyl radical cation were calculated for the AM1 structures and inspected (see Methodology). Figure 11 shows reproductions of the SOMOs for C1–C2 bond distances of 1.58, 1.75, and 2.2 Å. The SOMO at 1.75 Å corresponds to the TS on the UHF reaction path. It shows clearly that charge and spin are partially delocalized into the β-ring in the TS. These observations suggest that the barrier is mainly associated with establishing orbital overlap between the π- and σ-systems by stretching the C1–C2 bond. When sufficient
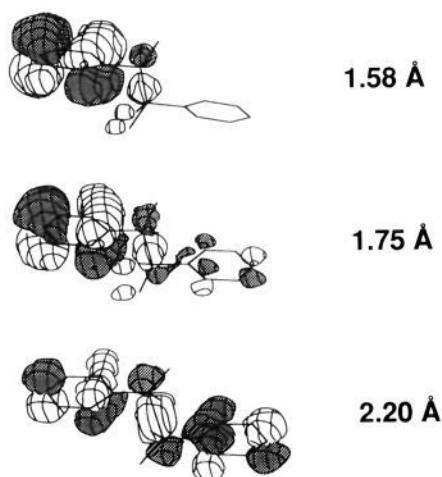
Figure 11. Singly occupied molecular orbital (SOMO) of bicumyl radical cation as a function of C1–C2 bond distance.

overlap is achieved, the charge developing at C1 and C2 as the bond is elongated can be stabilized by benzylic delocalization and inductive effects of the methyl groups.

For 1,2-diphenylethanol (DPE) radical cation, substitution of hydroxyl on the ethylene bridge gives a long-bond structure (potential energy minimum) that is about 8 kcal/mol less stable than the structure with normal C–C bond length (Figure 9). This structure apppears to be a loosely bound complex between benzyl radical and α-hydroxybenzyl cation. The TS between these two structures occurs at a C–C bond distance of 1.8 Å that corresponds approximately to the point where through-bond delocalization becomes significant in the dissociation of bibenzyl and bicumyl radical cations. The reason for a barrier between normal and long-bond structures of 1,2-diphenylethanol radical cation is similar to those provided in the above discussion on bicumyl radical cation. The long-bond structure derives its stability from delocalization of charge on to the hydroxyl group. It follows that the barrier is associated with distorting the σ-bonds enough to facilitate this delocalization. In this instance, the barrier is nearly equal to BDE, which again suggests that this transition from a π- to σ/π-radical cation is an important feature in radical-cation bond scission reactions.

Substituent Effects. The effects of substituents and structural variations on radical cation BDEs evidenced by these calculations are consistent with and complementary of experimental observations of one-electron oxidations of bibenzyl compounds.[3,6,7,10–15,25,29] Bibenzylic radical cations with *p*-methyl or *p*-hydroxyl groups have BDEs that are little different from bibenzyl radical cation (see Table II), but bibenzylic compounds with α-methyl or α-hydroxyl groups have substantially reduced radical cation BDEs, even to the point that C–C cleavage is predicted to be exothermic for bicumyl radical cation (see Table II). Yet, barriers to scission are predicted to exist and be associated with reorganizing the structure to enable through-bond delocalization. Once this is achieved, stabilizing interactions of the α-methyls in the developing cumyl cation–cumyl radical systems take the reaction on to products.

In recent experimental work, Maslak and Asel[15] have observed a novel substituent effect on the cleavage of 4-amino-4′-substituted-bicumyl radical cations. They observed that electron-donating substituents on the remote 4′-position accelerates C–C cleavage (ρ = −0.8 with use of σ⁺ constants). Since they report that ESR spectra of aminobicumyl radical cations are nearly identical with the ESR spectrum of *p*-(dimethylamino)-*tert*-butylbenzene radical cation reported by Drews et al.,[62] little through-space or through-bond delocalization is expected in the reactant geometries of these aminobicumyl radical cations. Thus,

(62) Drews, M. J.; Wong, P. S.; Jones, P. R. *J. Am. Chem. Soc.* **1972**, *94*, 9112.

the observed substituent effect must be manifested in the TS and not the reactant. Maslak and Asel[15] explain the substituent effect by describing the TS in valence-bond terms as an "interacting radical-cation pair", such that 4'-substituents are in benzylic resonance with positive charge that resides on C2: ArC$^+$--- •CAr' ↔ ArC• ---$^+$CAr'.

AM1 calculations for dissociation of bicumyl radical cation are consistent with these observations and explanation. The calculations suggest that the TS be thought of as a long-bond structure with through-bond delocalization between the phenyl groups. 4'-Substituents in such a structure interact directly with SOMO electron density to affect the TS stability while having negligible effect on the stability of the reactant (see Figure 11). For bicumyl radical cation, the TS is achieved very early with only partial delocalization into the β-ring. Aminobicumyl radical cations have greater barriers[15,63] to scission than bicumyl radical cation and are predicted by AM1 to have later TS with more developed through-bond delocalization.

Conclusions

The AM1 method can be useful for calculating radical-cation BDEs provided that one is cognizant that errors do not always cancel when calculated $\Delta H_f°$ for radicals, cations, and radical cations are combined. The errors are systematic and may be characterized by correlating calculated and experimental $\Delta H°_f$. Then, reasonably good agreement with experiment may be obtained by using this empirical relationship to correct calculated values for related structures and specie types. In this way, AM1 can be used to complement and augment thermochemical data and thereby enable BDEs or other reaction enthalpies to be estimated when experimental values are lacking or suspect.

The calculations suggest that reaction paths for scissions of radical cations may be differentiated by whether the scissions are endothermic or exothermic. Endothermic scissions, such as for bibenzyl radical cation, have loose, late-transition states with negligible barriers to recombination such that bonding interactions occur over relatively large distances. Exothermic scissions, such as for bicumyl radical cation, conversely have tight, early-transition states. The C–C bond in bicumyl radical cation is calculated to

break when elongated by as little as 10% of its equilibrium length.

In concurrence with Bellville et al.[38] long-bond structures with charge and spin delocalized through the central C–C bond are not predicted to be stable minima for bibenzylic radical cations. Evidently, any extra resonance stabilization that may accrue by through-bond delocalization between the two rings is more than offset by the energy necessary to distort the radical cation to attain good overlap for through-bond delocalization. The calculations suggest that long-bond structures are good transition-state models for exothermic bond scissions. As such, they may be key to understanding and predicting structure/reactivity trends.

Long-bond structures in energy minima should exhibit very different reactivities compared to π-type structures due to differences in charge distribution and geometry. Their intermediacy in chemical reactions might be inferred from appropriate kinetic and product studies. A recent observation by Dinnocenzo et al.[30] that ring opening of phenylcyclopropane radical cations is promoted by nucleophiles may be one such study. Also, long-bond structures could play a role in other than bond scission reactions. For example, endergonic electron-transfer reactions of bibenzylic or analogous compounds[64] could go via a long-bond TS. Here, the reduction in solvent reorganization energy achieved by greater delocalization of charge[65-67] in a long-bond TS structure might more than offset the reorganization energy for elongating the C–C bond.

(63) Camaioni, D. M. AM1 calculations to be published.

(64) Penn, J. H.; Deng, D.-L.; Chai, K.-J. *Tetrahedron Lett.* **1988**, *29*, 3636.
(65) See p 173 in: Eberson, L. *Adv. Phys. Org. Chem.* **1982**, *18*, 79–185.
(66) Gould, I. R.; Moser, J. E.; Ege, D.; Farid, S. *J. Am. Chem. Soc.* **1988**, *110*, 1990.
(67) Gould, I. R.; Ege, D.; Moser, J. E.; Farid, S. *J. Am. Chem. Soc.* **1990**, *112*, 4290.